Pulse Antenna Permutation and Pulse Antenna Modulation: Two Novel Diversity Schemes for Achieving Very High Data-Rates with Unipolar MIMO-UWB Communications

Chadi Abou-Rjeily, *Member IEEE*

***Abstract*—In this paper, we consider the problem of applying the Multiple-Input-Multiple-Output (MIMO) techniques on Impulse-Radio Time-Hopping Ultra-Wideband (IR-TH-UWB) communications. In particular, we propose two novel Space-Time (ST) block codes that are suitable for UWB. The proposed encoded MIMO-UWB schemes present the main advantage of conveying the information only through the positions of the very short unipolar UWB pulses. The constraint of unipolar transmissions keeps the transceiver structures very simple since it imposes no additional constraints on the RF circuitry to control the amplitudes or the phases of the sub-nanosecond UWB pulses. Consider the case where the transmitter is equipped with P antennas and where M PPM modulation positions are available. The first proposed scheme achieves a full transmit diversity order for $M \geq P$ while transmitting at the rate of $\log_2(M)$ bits Per Channel Use (PCU). The second scheme is fully diverse with any number of antennas and transmits at a rate of $M \log_2(P)/P$ bits PCU. The proposed codes permit to achieve different levels of compromise between complexity and performance since scheme 1 necessitates M-dimensional Maximum-Likelihood (ML) decoding while scheme 2 necessitates MP-dimensional decoding. We also present a comprehensive analysis on the enhancement in terms of the data rate achieved at a certain communication distance based on realistic indoor channel models and on an exact system model that takes inter-pulse-interference and inter-symbol-interference into consideration.**

***Index Terms*—MIMO, Ultra-WideBand (UWB), Space-Time (ST) coding, Pulse Position Modulation (PPM).**

I. Introduction and Motivation

Recently, Impulse-Radio (IR) Ultra-Wideband (UWB) emerged as a strong candidate for Wireless Personal Area Networks (WPANs). IR-UWB is a carrier-less transmission technique that gained increased popularity because of its capability of achieving high data rates with simple low-cost transceivers. However, the stringent power constraints imposed on the unlicensed UWB transmissions in different parts of the world [1] constitute the main limiting factor on the achievable rates and communication distances especially in Non-Line-Of-Sight (NLOS) scenarios. Consequently, advanced communication techniques are needed to overcome these limitations and to respond to the growing demand of various WPAN applications for data rate. In this context, several solutions proposed merging the Multiple-Input-Multiple-Output (MIMO) techniques with IR-UWB [2]–[8].

The author is with the department of Electrical and Computer Engineering of the Lebanese American University (LAU), Byblos, Lebanon (e-mail: chadi.abourjeily@lau.edu.lb).

Time-Hopping (TH) UWB systems are often associated with Pulse Position Modulation (PPM) where the information is conveyed by a sequence of time-shifted unipolar pulses. Unipolar transmission is appealing for TH-UWB since it is difficult to control the phases and amplitudes of the very low duty-cycle sub-nanosecond pulses used to convey the information symbols. On the other hand, while a huge amount of work considered the problem of Space-Time (ST) coding with QAM [9]–[11], the problem of ST coding with PPM is not very much explored.

Consider a single-user MIMO-UWB system equipped with P transmit antennas. Assume that M positions (or time slots) are available for data modulation within each symbol duration. M is often fixed by the complexity constraints on the transceiver since the dimensionality of the position-modulated constellation as well as the number of matched filters at the receiver both scale with M [6]. In this context, PPM ST codes can be classified into two categories. The first category of codes is unipolar where the information is conveyed exclusively by the time delays of pulses that can take only one amplitude level. The interest of unipolar codes resides in the fact that they introduce no additional constraints on the RF circuitry (especially on the pulse generators) compared to the corresponding single-antenna PPM systems. Unipolar codes can be either shape-preserving [7], [8] or non shape-preserving. Shape-preserving codes are appealing since, just as in the single-antenna systems, only one unipolar pulse is transmitted from each antenna during each symbol duration. In this context, the code proposed in [12] is shape-preserving with 2-PPM and non shape-preserving with M-PPM for $M > 2$. The second category of codes is non-unipolar and, in this case, the extension of the single-antenna PPM systems to the multi-antenna scenario necessitates transmitting pulses having different polarities and amplitude levels [2]–[6]. Evidently, non-unipolar codes break down the structure of the PPM constellation and increase the complexity of the transmitter. In this context, the different solutions that we propose in this paper are all unipolar.

The first contribution of the paper is that we propose a novel unipolar and shape-preserving rate-1 ST code that transmits at the rate of 1 symbol ($\log_2(M)$ bits) Per Channel Use (PCU) with M-PPM. This scheme will be referred to as scheme 1 in what follows. Scheme 1 can achieve a full transmit diversity order with M-PPM constellations and P

transmit antennas for all values of $M \geq P$. Scheme 1 shares the same interesting properties as the PPM-codes proposed in [7], [8]. Namely, scheme 1 as well as [7], [8] are all unipolar, shape-preserving and transmit at the same rate of $\log_2(M)$ bits PCU. The superiority of the proposed scheme over [7], [8] can be summarized in the following points. (1): Scheme 1 can be applied for a wider range of (P, M) (in particular for all values of P satisfying $P \leq M$ compared to the values of (P, M) given in table-1 in [8]). For example, scheme 1 is the first known unipolar shape-preserving code that can be applied with the following values of (P, M): $(P, M) \in \{(p, m)\ ;\ p = 3, 4\ ;\ m = 4\} \cup \{(p, m)\ ;\ p = 5, 6\ ;\ m = 6, 8\} \cup \{(p, m)\ ;\ p = 7, 8\ ;\ m = 8, 9, 10, 12\}$. (2): Scheme 1 requires a simpler decoding complexity compared to [7], [8] since the decoding procedure involves M dimensions rather than PM dimensions as in [7], [8]. (3): In contrast to all fully diverse ST codes that extend over at least P symbol durations, scheme 1 extends over only one symbol duration thus reducing the decoding delays at the receiver side. Note that ST coding over one symbol duration is rendered possible because of the particular structure of the PPM signal set as will be explained later.

On the other hand, a key solution that was adopted in the literature for exceeding the rate of 1 symbol PCU achieved by rate-1 QAM ST codes consisted of introducing a constellation expansion to the uncoded signal set [10], [11]. Such constellation expansions often consist of either amplitude (or phase) scaling [10] or of algebraic rotations [11]. For PPM, the idea of constellation expansion was applied in [6] to propose a family of full-rate ST codes that is based on pulse permutations and algebraic rotations. Even though [6] transmits at a rate that exceeds 1 symbol ($\log_2(M)$ bits) PCU with M-PPM, the introduced algebraic rotations render this scheme non unipolar.

In this context, the second contribution of the paper consists of proposing the first known ST code that is capable of transmitting at a rate that exceeds $\log_2(M)$ bits PCU while maintaining unipolar transmissions. In particular, this scheme (that will be referred to as scheme 2 in what follows) transmits at the rate of $M \log_2(P)/P$ bits PCU. Given that practical MIMO systems are often equipped with a limited number of antennas (because of the cost constraints) while the number of modulation positions M can take relatively large values, then the rate of scheme 2 often exceeds the limit of $\log_2(M)$ bits PCU especially for large values of M. For example, with $P = 2$ transmit antennas and $M = 32$ modulation positions, scheme 2 transmits 3.2 times faster than the rate-1 PPM codes ([7], [8] and scheme 1) and 1.6 times faster than the full-rate codes proposed in [6]. Note that these high multiplexing gains are associated with an enhanced diversity order since scheme 2 is fully diverse for all values of P and M.

As a conclusion, comparing scheme 2 with the other unipolar codes, it can be seen that the advantages of scheme 2 over [7], [8] reside in a potentially higher data rate especially for large values of M and in the fact that scheme 2 can be applied for all values of (P, M) with the same decoding complexity (PM-dimensional decoders are required). The superiority of scheme 2 over [6] can be summarized in the following points. (1): Unlike [6], scheme 2 can be applied with all values of P and M. (2): As will be explained later, scheme 2 is based on a time domain constellation expansion rather than an amplitude domain expansion making it capable of maintaining unipolar transmissions. (3): The rate of scheme 2 (resp. [6]) increases linearly (resp. logarithmically) with M and, consequently, scheme 2 can achieve much higher data rates for large values of M. (4): Scheme 2 admits a simpler decoding complexity since it can be associated with PM-dimensional decoders rather than P^2M-dimensional decoders as [6].

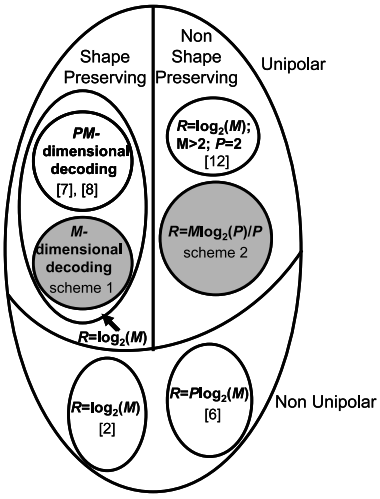

Fig. 1. ST codes for M-PPM with P transmit antennas. R stands for the normalized data rate in bits PCU. The proposed solutions are represented by shaded sets.

Fig. 1 shows the different classes of PPM ST codes. The proposed schemes are described schematically in Fig. 2. In this figure, we also show the schematic representation of spatial multiplexing for comparison. Note that one M-PPM symbol and its permutated versions are transmitted from the different antennas in scheme 1 that will be referred to as pulse antenna permutation. In scheme 2, one antenna is pulsed during each modulation position and this scheme will be referred to as pulse antenna modulation (in analogy with pulse position modulation). Note that in scheme 2, the index of the antenna that is pulsed is permuted among the P symbol durations.

Notations: $\mathbf{1}_{m\times n}$ and $\mathbf{0}_{m\times n}$ correspond to the $m \times n$ matrices whose elements are all equal to 1 and 0 respectively. e_m stands for the m-th column of the $M \times M$ identity matrix I_M. $\otimes$ stands for the Kronecker product and $\delta_{i,j}$ stands for Kronecker's delta function. The function vec(X) stands for stacking the columns of the matrix X vertically one after the other. The function $\lceil x \rceil$ rounds the real number x to the nearest integer that is greater than or equal to it.

II. SYSTEM MODEL

A. Basic Parameters

A general expression of the signal transmitted from the p-th antenna is given by:

$$s_p(t) = \frac{1}{\sqrt{PN_f}} \sum_{j=1}^{\infty} \sum_{m=1}^{M} a_{p,j,m} \sum_{n=1}^{N_f} w(t - (j-1)T_s - (n-1)T_f - c_n T_c - (m-1)\delta) \quad (1)$$

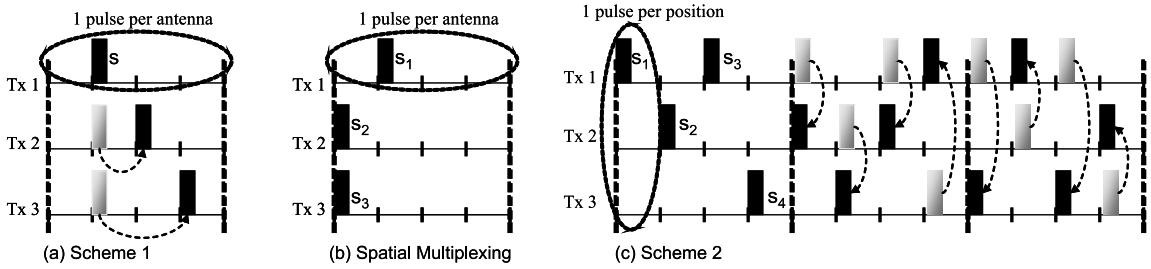

Fig. 2. Schematic representation with $P = 3$ transmit antennas and $M = 4$ modulation positions. (a): Scheme 1 with $s = 2 \in \{1, \ldots, M\}$. (b): Spatial-Multiplexing with $s_1 = 2$ and $s_2 = s_3 = 1$; note that $s_p \in \{1, \ldots, M\}$ for $p = 1, \ldots, P$. (c): Scheme 2 with $s_1 = 1$, $s_2 = 2$, $s_3 = 1$ and $s_4 = 3$; note that $s_m \in \{1, \ldots, P\}$ for $m = 1, \ldots, M$. (a) and (b) extend over 1 symbol duration while (c) extends over 3 symbol durations.

where the multiplying factor $\frac{1}{\sqrt{P}}$ was introduced in order to have the same total transmitted energy as in the case of single-antenna systems. In eq. (1):

- $a_{p,j,m} = 1$ (resp. $a_{p,j,m} = 0$) stands for the presence (resp. absence) of a pulse emitted from the p-th transmit antenna during the m-th PPM position of the j-th symbol duration.
- $w(t)$ is the pulse waveform of duration T_w and it is normalized to have a unit energy.
- δ is the PPM modulation delay chosen to verify: $\delta \geq T_w$.
- N_f is the number of time-hopped pulses used to transmit one information symbol, T_f is the average separation between two consecutive pulses and $T_s = N_f T_f$ is the symbol duration.
- $c_n \in \{0, \ldots, N_c - 1\}$ is the additional time shift (normalized by T_c) applied on the pulses transmitted by the considered user during the n-th frame of each symbol duration. T_c is the chip duration and N_c is the number of chips per frame (of duration T_f). In order to result in the same average multi-user interference as in the single-antenna case, all antennas of the same user are assumed to share the same pseudo-random TH sequence. Moreover, this sequence will be assumed to be periodic with period N_f.

Denote by Γ the maximum delay spread of the underlying UWB channel ($\Gamma \gg T_w$), Inter-Frame-Interference (IFI) and, consequently, Inter-Symbol-Interference (ISI) can be eliminated by choosing:

$$T_f \geq \Gamma + N_c T_c + (M-1)\delta + T_w \tag{2}$$

In the same way, the interference between the different modulation positions (referred to as IPI for Inter-Pulse-Interference) can be eliminated if the modulation delay satisfies the relation:

$$\delta \geq \Gamma + T_w \tag{3}$$

Note that the absence of IPI implies the absence of IFI and ISI as well.

B. System Model

We assume that the receiver is equipped with Q antennas and that each antenna is followed by an L-th order Rake receiver that combines the L first arriving multi-path components.

In what follows, the indices $q \in \{1, \ldots, Q\}$, $p \in \{1, \ldots, P\}$ and $l \in \{1, \ldots, L\}$ will correspond to the receive antenna, transmit antenna and the Rake finger respectively. In the same way, $j \in \{1, \ldots, J\}$ stands for the symbol index, $n \in \{1, \ldots, N_f\}$ for the frame index and $m \in \{1, \ldots, M\}$ for the PPM position index. In what follows, we consider the case where the information is mapped into ST codewords that extend over J symbol durations.

From eq. (1), the signal received at the q-th antenna can be written as:

$$r_q(t) = \sum_{p=1}^{P} \sum_{j=1}^{\infty} \sum_{m=1}^{M} a_{p,j,m} \sum_{n=1}^{N_f} h'_{q,p}(t - (j-1)T_s - (n-1)T_f - c_n T_c - (m-1)\delta) + n_q(t) \tag{4}$$

where $h'_{q,p}(t)$ stands for the convolution of $w(t)$ with the impulse response of the channel between antennas p and q and $n_q(t)$ is the noise at the q-th antenna and it is assumed to be real AWGN. Note that the normalizing factor $\sqrt{PN_f}$ in eq. (1) was omitted for simplicity; in fact, this term can be included in the variance of $n_q(t)$ which is equal to $PN_fN_0/2$ (where N_0 stands for the noise spectral density).

The receiver consists of a bank of correlators that collect $JQLN_fM$ decision variables during the duration of each codeword. These decision variables are given by:

$$y_{j,q,l,n,m} = \int_0^{T_f} r_q(t) \widetilde{w}_{j,l,n,m}(t) \mathrm{d}t \tag{5}$$

where $\widetilde{w}_{j,l,n,m}(t)$ is a reference signal given by:

$$\widetilde{w}_{j,l,n,m}(t) = w\left(t - (j-1)T_s - \Delta_l - (n-1)T_f - c_n T_c - (m-1)\delta\right) \tag{6}$$

where $\Delta_l \triangleq (l-1)T_w$ corresponds to the delay of the l-th Rake finger.

Replacing eq. (4) in eq. (5) results in:

$$y_{j,q,l,n,m} = \sum_{p'=1}^{P} \sum_{j'=1}^{\infty} \sum_{n'=1}^{N_f} \sum_{m'=1}^{M} a_{p',j',m'} h_{q,p'} \left[(j-j')T_s + \Delta_l + (n-n')T_f + (c_n - c_{n'})T_c + (m-m')\delta\right] + n_{j,q,l,n,m} \tag{7}$$

where $n_{j,q,l,n,m} = \int_0^{T_f} n_q(t) \widetilde{w}_{j,l,n,m}(t) \mathrm{d}t$ and:

$$h_{q,p}(\tau) = \int_0^{T_f} h'_{q,p}(t) w(t-\tau) \mathrm{d}t \tag{8}$$

The ST encoding scheme will be determined by the choice of the $PM \times J$ codeword A whose $((p-1)M+m, j)$-th entry is equal to $a_{p,j,m}$. In what follows, we denote by $\mathcal{A}$ the PMJ-dimensional vector given by: $\mathcal{A} = \text{vec}(A)$.

At a first time, we ignore the interference among the different codewords. Based on the above notations, the linear dependence between the baseband inputs and outputs of the channel can be expressed as:

$$\mathcal{Y} = \mathcal{H}^{(0)} \left[I_{PJ} \otimes \left(\mathbf{1}_{N_f \times 1} \otimes I_M \right) \right] \mathcal{A} + \mathcal{N} \tag{9}$$

where $\mathcal{Y}$ is the decision vector of length $JQLN_fM$ such that:

$$\begin{aligned} \mathcal{Y}\,[&(j-1)QLN_fM + (q-1)LN_fM \\ &+ (l-1)N_fM + (n-1)M + m] = y_{j,q,l,n,m} \end{aligned} \tag{10}$$

and $\mathcal{N}$ is the noise vector that is constructed in the same way as $\mathcal{Y}$.

In eq. (9), $\mathcal{H}^{(0)}$ is the $JQLN_fM \times JPN_fM$ channel matrix given by:

$$\mathcal{H}^{(0)} = \begin{bmatrix} \mathcal{H}_1 & \mathbf{0}_{QLN_fM \times PN_fM} & \cdots & \mathbf{0}_{QLN_fM \times PN_fM} \\ \mathcal{H}_2 & \mathcal{H}_1 & \ddots & \vdots \\ \vdots & \ddots & \ddots & \mathbf{0}_{QLN_fM \times PN_fM} \\ \mathcal{H}_J & \cdots & \mathcal{H}_2 & \mathcal{H}_1 \end{bmatrix} \tag{11}$$

where $\mathcal{H}_j$ quantifies the interference (IFI and ISI) between two columns of the same codeword that are separated by $(j-1)$ symbol durations. $\mathcal{H}_j$ is a $QLN_fM \times PN_fM$ block matrix whose (q,p)-th block is denoted by $\mathcal{H}_{j,q,p}$ for $q = 1, \ldots, Q$ and $p = 1, \ldots, P$. $\mathcal{H}_{j,q,p}$ is a $LN_fM \times N_fM$ matrix that can be written as: $\mathcal{H}_{j,q,p} = [\mathcal{H}^T_{j,q,p,1} \ \cdots \ \mathcal{H}^T_{j,q,p,L}]^T$ where $\mathcal{H}_{j,q,p,l}$ is a $N_fM \times N_fM$ block matrix whose (n,n')-th $(M \times M)$-dimensional block is denoted by $\mathcal{H}_{j,q,p,l,n,n'}$ for $n, n' = 1, \ldots, N_f$. The (m,m')-th element of $\mathcal{H}_{j,q,p,l,n,n'}$ is given by:

$$h_{q,p}\left((j-1)T_s + \Delta_l + (n-n')T_f + (c_n - c_{n'})T_c + (m-m')\delta\right) \tag{12}$$

Each codeword can interfere with N_{in} codewords where:

$$N_{in} = \left\lceil \frac{\Gamma - (T_f - N_cT_c - (M-1)\delta - T_w)}{JN_fT_f} \right\rceil \tag{13}$$

Including the interference among the different codewords, eq. (9) will be modified to:

$$\begin{aligned} \mathcal{Y} = &\mathcal{H}^{(0)} \left[I_{PJ} \otimes \left(\mathbf{1}_{N_f \times 1} \otimes I_M \right) \right] \mathcal{A} \\ &+ \mathcal{H}^{(in)} \left[I_{PJN_{in}} \otimes \left(\mathbf{1}_{N_f \times 1} \otimes I_M \right) \right] \mathcal{A}^{(in)} + \mathcal{N} \end{aligned} \tag{14}$$

where $\mathcal{A}^{(in)}$ is a vector of length $N_{in}JPM$. It is given by: $\mathcal{A}^{(in)} = [[\mathcal{A}(N_{in})]^T \ \cdots \ [\mathcal{A}(1)]^T]^T$ where $\mathcal{A}(i)$ stands for the vector of length JPM obtained from the vertical concatenation of the columns of the codeword that precedes the considered codeword by iJ symbol durations. Based on this notation, the vector $\mathcal{A}$ in eq. (14) can be written as $\mathcal{A} = \mathcal{A}(0)$.

In eq. (14), $\mathcal{H}^{(in)}$ is a $JQLN_fM \times N_{in}JPN_fM$ matrix given by: $\mathcal{H}^{(in)} = [\mathcal{H}(N_{in}) \ \cdots \ \mathcal{H}(1)]$ where $\mathcal{H}(i)$ is given by:

$$\mathcal{H}(i) = \begin{bmatrix} \mathcal{H}_{iJ+1} & \mathcal{H}_{iJ} & \cdots & \mathcal{H}_{iJ-(J-2)} \\ \mathcal{H}_{iJ+2} & \mathcal{H}_{iJ+1} & \ddots & \vdots \\ \vdots & \ddots & \ddots & \mathcal{H}_{iJ} \\ \mathcal{H}_{(i+1)J} & \cdots & \mathcal{H}_{iJ+2} & \mathcal{H}_{iJ+1} \end{bmatrix} \tag{15}$$

where the construction of the $QLN_fM \times PN_fM$ matrix $\mathcal{H}_j$ is as described above. From eq. (12), it follows that $\mathcal{H}_j$ will be equal to the all-zero matrix when $j < 1$. Based on this notation, the channel matrix $\mathcal{H}^{(0)}$ in eq. (11) can be written as: $\mathcal{H}^{(0)} = \mathcal{H}(0)$.

C. Simplified System Model in the Absence of Interference

From the previous subsection, it is evident that the model of MIMO UWB systems described in eq.(14) is intractable and does not lend itself to a simple analytical analysis. Therefore, we adopt the following approach in our work. First, we consider the problem of ST code design in the absence of IPI. This first step is convenient for determining and understanding the main characteristics of the proposed schemes; especially the achieved transmit diversity order. Even though, the code design is based on the simple scenario of no IPI, the analysis that we present on the coverage extension offered by MIMO-UWB systems in section IV as well as all simulation results will be based on the exact model presented subsection II-B and that takes into account IPI, IFI and ISI. This approach is equivalent to assuming that interference can be considered as a perturbation on the proposed schemes. This assumption will be further justified and strengthened in section III where we present the different code constructions.

In this subsection, we present a simplified system model in the absence of IPI. On the other hand, the solutions that we propose do not depend on the value taken by N_f and, consequently, unlike [2] can be applied with very high data-rate UWB systems that do not employ any pulse repetitions ($N_f = 1$). Since N_f has no impact on the performance of the proposed ST codes in the absence of interference, we also assume that $N_f = 1$ in this model for the sake of simplicity.

In the absence of ISI, the constituent sub-matrices $\mathcal{H}_j$ of the channel matrix $\mathcal{H}^{(0)}$ in eq. (11) will be equal to the all-zero matrix when $j \neq 1$. Consequently, $\mathcal{H}^{(0)}$ can be written as: $\mathcal{H}^{(0)} = I_J \otimes \mathcal{H}_1$. Denoting $\mathcal{H}_1$ by $\mathcal{H}$, eq. (14) can be written as:

$$\mathcal{Y} = [I_J \otimes \mathcal{H}]\, \mathcal{A} + \mathcal{N} \tag{16}$$

On the other hand, for $N_f = 1$ and $j = 1$, the channel coefficients in eq. (12) reduce to:

$$h_{q,p}\left((\Delta_l + (m-m')\delta\right) = h_{q,p}\left(\Delta_l\right)\delta_{m,m'} \tag{17}$$

where $\delta_{i,j}$ corresponds to Kronecker's delta function and the second equality follows from the condition of no IPI.

Therefore, in the absence of IPI and for $N_f = 1$, the $QLM \times PM$ channel matrix $\mathcal{H}$ in eq. (16) can be written as:

$$\mathcal{H} = H \otimes I_M \tag{18}$$

where H is a $QL \times P$ matrix whose $((q-1)L + l, p)$-th element is denoted by $h_{q,l,p}$ for $q = 1, \ldots, Q$, $l = 1, \ldots, L$

and $p = 1, \ldots, P$. From eq. (8) and eq. (17), $h_{q,l,p}$ is given by:

$$h_{q,l,p} = h_{q,p}(\Delta_l) = \int_0^{T_f} h'_{q,p}(t) w(t - \Delta_l) \mathrm{d}t \tag{19}$$

III. Codes Constructions

As indicated before, the model given in eq. (16) will be used for the code construction in this section while all of the numerical results will be based on the exact model presented in eq. (14).

A. Scheme 1: Pulse Antenna Permutation

The first diversity scheme is based on pulse permutations and extends over $J = 1$ symbol duration only. For simplicity, since $J = 1$, the pulse positions $a_{p,j,m}$ can be denoted by $a_{p,m}$ for $p = 1, \ldots, P$ and $m = 1, \ldots, M$.

Denote by $s \in \{1, \ldots, M\}$ the position of a M-ary PPM information symbol. The transmission strategy corresponds to fixing:

$$a_{p,m} = \delta_{\pi^{p-1}(s),m} \quad ; \quad p = 1, \ldots, P \tag{20}$$

where $\pi^k(.)$ stands for the cyclic permutation of order k given by:

$$\pi^k(i) = (i + k - 1) \mod M + 1 \tag{21}$$

In other words, the first antenna transmits only one pulse during the s-th modulation position while the p-th antenna transmits one pulse that is cyclically permutated by $p - 1$ positions for $p = 2, \ldots, P$. Evidently, this scheme introduces no expansion to the M-PPM constellation since each antenna transmits only one unipolar pulse during one out of the M available positions.

The most appealing feature of this diversity scheme is its simplicity since only one M-PPM information symbol is involved in the encoding and decoding procedures. Moreover, this simplicity is achieved with no penalty on the data rate since scheme 1 is a rate-1 ST code that transmits at the rate of 1 M-PPM symbol ($\log_2(M)$ bits) Per Channel Use (PCU).

Unlike all of the existing ST codes that extend over at least $J = P$ symbol durations, scheme 1 profits from an enhanced diversity order by conveniently encoding the positions of the unipolar pulses transmitted during $J = 1$ symbol duration as stated in the next proposition.

Proposition 1: For P transmit antennas, scheme 1 achieves a full transmit diversity order with M-PPM constellations for the values of M satisfying: $M \geq P$.

Proof: For scheme 1, the codeword $\mathcal{A}$ in eq. (16) reduces to a PM-dimensional vector that can be written as: $\mathcal{A} = [e_s^T, e_{\pi(s)}^T, \ldots, e_{\pi^{P-1}(s)}^T]^T$ where e_m stands for the m-th column of the $M \times M$ identity matrix I_M. In an equivalent way, $\mathcal{A}$ can be written as: $\mathcal{A} = \Phi S$ where $S \triangleq e_s$ and Φ is the $PM \times M$ matrix given by:

$$\Phi = \begin{bmatrix} I_M & \left(\Omega^1\right)^T & \cdots & \left(\Omega^{P-1}\right)^T \end{bmatrix}^T \tag{22}$$

where Ω is the $M \times M$ cyclic permutation matrix given by:

$$\Omega = \begin{bmatrix} \mathbf{0}_{1\times(M-1)} & 1 \\ I_{M-1} & \mathbf{0}_{(M-1)\times 1} \end{bmatrix} \tag{23}$$

where $\mathbf{0}_{m\times n}$ is the all-zero $m \times n$ matrix.

The Maximum-Likelihood (ML) decoder decides in the favor of vector S that minimizes:

$$\|\mathcal{Y} - \mathcal{H}\Phi S\|^2 = \mathcal{Y}^T\mathcal{Y} - 2\mathcal{Y}^T\mathcal{H}\Phi S + S^T\Phi^T\mathcal{H}^T\mathcal{H}\Phi S \tag{24}$$

where from eq. (18): $\mathcal{H}^T\mathcal{H} = (H \otimes I_M)^T (H \otimes I_M) = H^T H \otimes I_M$ following from the properties of the Kronecker product. In what follows, we denote by G the $P \times P$ symmetric matrix given by: $G = H^T H$. From eq. (19), it can be easily seen that the (p, p')-th element of G is given by:

$$G(p, p') \triangleq g_{p,p'} = \sum_{q=1}^{Q} \sum_{l=1}^{L} h_{q,l,p} h_{q,l,p'} \tag{25}$$

On the other hand, eq. (23) implies that Ω^i is a unitary matrix whose transpose is given by Ω^{-i}. Consequently, from eq. (22), $\Phi^T = \begin{bmatrix} I_M & \Omega^{-1} & \cdots & \Omega^{-(P-1)} \end{bmatrix}$. Therefore, after some manipulations, the matrix $\Phi^T\mathcal{H}^T\mathcal{H}\Phi$ in eq. (24) can be written as:

$$\Phi^T\mathcal{H}^T\mathcal{H}\Phi = \sum_{i=1}^{P} \Omega^{-(i-1)} \sum_{j=1}^{P} g_{i,j}\Omega^{j-1} = \sum_{i=1}^{P}\sum_{j=1}^{P} g_{i,j}\Omega^{j-i} \tag{26}$$

As stated in the proposition, we limit ourselves to the case $P \leq M$. The reason for this choice will become clearer at the end of this subsection. Consequently, eq. (26) can be written as:

$$\Phi^T\mathcal{H}^T\mathcal{H}\Phi = \sum_{i=1}^{M}\sum_{j=1}^{M} g_{i,j}\Omega^{j-i} \tag{27}$$

$$= \sum_{i=1}^{M} \left[g_{i,i} I_M + \sum_{j=i+1}^{M} g_{i,j}\Omega^{j-i} + \sum_{j=1}^{i-1} g_{i,j}\Omega^{j-i} \right] \tag{28}$$

where $g_{i,j}$ is given in eq. (25) for $(i, j) \in \{1, \ldots, P\}^2$ and $g_{i,j} = 0$ for $(i, j) \in \{P + 1, \ldots, M\}^2$.

By a change of variable, the first summation in eq. (28) can be written as: $\mathcal{I}_1 \triangleq \sum_{j=i+1}^{M} g_{i,j}\Omega^{j-i} = \sum_{j=1}^{M-i} g_{i,i+j}\Omega^j$. In the summation $\mathcal{I}_1$, $j \leq M - i$ implying that $j < M - i + 1$. Consequently, $i + j - 1 < M$ and from eq. (21):

$$\pi^j(i) = (i + j - 1) \mod M + 1 = (i + j - 1) + 1 = i + j \tag{29}$$

consequently, summation $\mathcal{I}_1$ can be written as: $\mathcal{I}_1 = \sum_{j=1}^{M-i} g_{i,\pi^j(i)}\Omega^j$.

Denote by $\mathcal{I}_2$ the second summation in eq. (28). Since $\Omega^M = I_M$, then $\mathcal{I}_2 \triangleq \sum_{j=1}^{i-1} g_{i,j}\Omega^{j-i} = \sum_{j=1}^{i-1} g_{i,j}\Omega^{j-i+M}$. By a change of variable, this summation can be written as: $\mathcal{I}_2 = \sum_{j=M-i+1}^{M-1} g_{i,i+j-M}\Omega^j$. In this summation, $j \geq M - i + 1$ implying that $i + j - 1 \geq M$. Therefore, from eq. (21):

$$\begin{aligned} \pi^j(i) &= (i + j - 1) \mod M + 1 \\ &= (i + j - 1 - M) + 1 = i + j - M \end{aligned} \tag{30}$$

consequently, summation $\mathcal{I}_2$ can be written as: $\mathcal{I}_2 = \sum_{j=M-i+1}^{M-1} g_{i,\pi^j(i)}\Omega^j$.

Therefore, eq. (28) can be written as:

$$\Phi^T\mathcal{H}^T\mathcal{H}\Phi = \sum_{i=1}^{M}\left[g_{i,i}I_M + \sum_{j=1}^{M-1} g_{i,\pi^j(i)}\Omega^j\right] \quad (31)$$

$$= I_M\left[\sum_{i=1}^{M} g_{i,i}\right] + \sum_{j=1}^{M-1}\Omega^j\left[\sum_{i=1}^{M} g_{i,\pi^j(i)}\right] \quad (32)$$

Applying the change of variable $j' = -j+M$ on the second summation of the last equation results in:

$$\Phi^T\mathcal{H}^T\mathcal{H}\Phi = I_M\left[\sum_{i=1}^{M} g_{i,i}\right] + \sum_{j=1}^{M-1}\Omega^{-j+M}\left[\sum_{i=1}^{M} g_{i,\pi^{-j+M}(i)}\right] \quad (33)$$

$$= I_M\left[\sum_{i=1}^{M} g_{i,i}\right] + \sum_{j=1}^{M-1}\left(\Omega^T\right)^j\left[\sum_{i=1}^{M} g_{i,\pi^{-j}(i)}\right] \quad (34)$$

where the last equation follows since $\Omega^M = I_M$, $\Omega^{-1} = \Omega^T$ and since $\pi^M(m) = m$ for $m = 1, \ldots, M$.

Equation (34) can be written as:

$$\Phi^T\mathcal{H}^T\mathcal{H}\Phi = \alpha I_M + \sum_{j=1}^{M-1}\beta_j\left(\Omega^T\right)^j \quad (35)$$

where:

$$\alpha \triangleq \sum_{i=1}^{M} g_{i,i} = \sum_{i=1}^{P} g_{i,i} = \sum_{i=1}^{P}\sum_{q=1}^{Q}\sum_{l=1}^{L} h_{q,l,i}^2 \quad (36)$$

$$\beta_j \triangleq \sum_{i=1}^{M} g_{i,\pi^{-j}(i)} = \sum_{i=1}^{P} g_{i,\pi^{-j}(i)} = \sum_{i=1}^{P}\sum_{q=1}^{Q}\sum_{l=1}^{L} h_{q,l,i}h_{q,l,\pi^{-j}(i)} \quad (37)$$

where the above equations follow from eq. (25) and from the fact that $g_{i,i} = 0$ and $g_{i,\pi^{-j}(i)} = 0$ for $i > P$ by construction.

The elements of $\left(\Omega^T\right)^j$ are equal to 1 on the j-th upper diagonal and $(M-j)$-th lower diagonal and are equal to zero elsewhere. Consequently, $\left(\Omega^T\right)^j$ can not be equal to I_M for $j = 1 \ldots M-1$. Therefore, from eq. (35), the diagonal elements of $\Phi^T\mathcal{H}^T\mathcal{H}\Phi$ are all equal to α.

In eq. (24), since the vector S (which is the vector representation of a M-PPM symbol) is equal to a certain column of I_M, then $S^T\Phi^T\mathcal{H}^T\mathcal{H}\Phi S$ is always equal to a diagonal element of $\Phi^T\mathcal{H}^T\mathcal{H}\Phi$. From what preceded, since all the diagonal elements of $\Phi^T\mathcal{H}^T\mathcal{H}\Phi$ are equal, then a ML decoding rule equivalent to eq. (24) is given by:

$$\hat{s} = \arg\max_{s\in\{1,\ldots,M\}}\left[\mathcal{Y}^T\mathcal{H}\Phi e_s\right] \quad (38)$$

Consider the high signal-to-noise ratio (SNR) regime and assume that the PPM symbol $s_0 \in \{1, \ldots, M\}$ was transmitted, then $\mathcal{Y} = \mathcal{H}\Phi e_{s_0}$ resulting in:

$$\hat{s} = \arg\max_{s\in\{1,\ldots,M\}}\left[e_{s_0}^T\Phi^T\mathcal{H}^T\mathcal{H}\Phi e_s\right] \quad (39)$$

On the other hand, $e_{s_0}^T\Phi^T\mathcal{H}^T\mathcal{H}\Phi e_s$ is equal to the (s_0, s)-th element of $\Phi^T\mathcal{H}^T\mathcal{H}\Phi$. Based on the structure of $\Phi^T\mathcal{H}^T\mathcal{H}\Phi$ given in eq. (35), it follows that:

$$e_{s_0}^T\Phi^T\mathcal{H}^T\mathcal{H}\Phi e_s = \begin{cases}\alpha, & s = s_0;\\ \beta_{|s_0-s|}, & s \neq s_0.\end{cases} \quad (40)$$

where α and $\beta_{|s_0-s|}$ can be obtained from equations (36) and (37) respectively. Note that from eq. (37), β_j contains at most QLP non-zero terms since $g_{i,\pi^{-j}(i)} = 0$ when $\pi^{-j}(i) > P$.

From equations (36) and (40), it follows that at high SNRs $\alpha \ll 1$ (and consequently the PPM symbol s_0 is lost) if and only if $|h_{q,l,p}| \ll 1$ for $q = 1, \ldots, Q$, $L = 1, \ldots, L$ and $p = 1, \ldots, P$. In other words, the information symbol is lost only when the PQ sub-channels suffer from fading over a duration LT_w. Therefore, the proposed scheme achieves full transmit, receive and multi-path diversities.

The next argument will also show that the proposed scheme guides the receiver in the sense of making correct decisions as P increases. Note that in eq. (40), α corresponds to a correct decision while β_j corresponds to confusing the transmitted position with a position that is j slots further (in a cyclic pattern). Since α can be written as $\alpha = \beta_0$ and since $\pi^{-j}(i) \neq i$ for $j = 1, \ldots, M-1$, then $\beta_j < \alpha$ for $j = 1, \ldots, M-1$ following from the properties of the autocorrelation function. For a fixed value of (Q, L), note that α (and consequently the diagonal elements of $\Phi^T\mathcal{H}^T\mathcal{H}\Phi$) adds up coherently as P increases. On the other hand, β_j for $j = 1, \ldots, M-1$ (and consequently all the non-diagonal elements of $\Phi^T\mathcal{H}^T\mathcal{H}\Phi$) do not contain any squared channel coefficient since $h_{q,l,i} \neq h_{q,l,\pi^{-j}(i)}$ following from $\pi^{-j}(i) \neq i$ for $j = 1, \ldots, M-1$. As a conclusion, the gap between the absolute values of the diagonal elements (corresponding to correct decisions) and the non-diagonal elements (corresponding to erroneous decisions) increases with P thus enhancing the diversity order of the proposed scheme and making it more resistent to errors.

While in the above analysis the diversity order was investigated in the absence of IPI, the impact of IPI will manifest itself in the presence of additional cross terms that will be added to α and β_j in eq. (40). Since these cross terms can be positive or negative with the same probability, then their average will tend to zero. Moreover, these interference terms do not add up coherently and, consequently, their effect can be considered as a perturbation on α (and, consequently, on the overall diversity order of the system).

B. Scheme 2: Pulse Antenna Modulation

Single-antenna systems, scheme 1 as well as the shape-preserving PPM codes [7], [8] all correspond to transmitting one pulse during one out of the M available modulation positions. The novel idea that we propose in this section is as follows: during each modulation position, only one transmit antenna (out of the P antennas) is allowed to transmit an information-carrying pulse. In other words, instead of modulating the information symbols over the M PPM positions for each transmit antenna p ($p = 1, \ldots, P$), these symbols are modulated over the P transmit antennas for each modulation position m ($m = 1, \ldots, M$). Evidently, the proposed scheme is exclusive to MIMO systems.

Designate by $s_1, \ldots, s_M \in \{1, \ldots, P\}$ M P-ary symbols. The diversity scheme that we propose extends over $J = P$ symbol durations and is given by:

$$a_{p,j,m} = \delta_{p,\sigma^{j-1}(s_m)} \;\; ; \;\; p = 1 \ldots P; j = 1 \ldots J; m = 1 \ldots M \quad (41)$$

where $\sigma^k(.)$ stands for the cyclic permutation of order k (among the P transmit antennas) given by:

$$\sigma^k(i) = (i + k - 1) \mod P + 1 \quad (42)$$

In other words, for a given modulation position m, antenna $\sigma^{j-1}(s_m)$ is pulsed during the j-th symbol duration. From eq. (41), it follows that the number of bits transmitted PCU is:

$$\mathcal{R}_2 = \frac{M \log_2(P)}{P} \quad (43)$$

while the rate of scheme 1 (and of all the existing shape-preserving PPM codes) is $\mathcal{R}_1 = \log_2(M)$ bits PCU. Given that practical systems are equipped with a limited number of antennas, then M is often much greater than P and scheme 2 presents the main advantage of an enhanced data rate with respect to scheme 1. For example, for modulation over 16 positions with 2 transmit antennas, scheme 2 transmits two times faster than scheme 1.

Unlike spatial-multiplexing systems where the data rate is increased at the expense of sacrificing the transmit diversity order, the increase in data rate that results from scheme 2 is accompanied with an enhanced diversity order as stated in the next proposition. Finally, since for scheme 2 in the average M/P pulses are transmitted from each antenna, the waveform $w(t)$ in eq. (1) must be normalized by $\sqrt{P/M}$ to ensure the same transmission level compared to SISO M-PPM systems.

Proposition 2: For $P > 1$ transmit antennas, scheme 2 achieves a full transmit diversity order with M-PPM constellations for all the values M.

Proof: The proof is provided in the appendix.

From proposition 1 and proposition 2, it follows that one advantage of scheme 2 over scheme 1 resides in the fact that the former can be applied for all values of (P, M) while the latter is limited to $M \geq P$. On the other hand, scheme 2 presents the disadvantage of an increased decoder complexity since M P-ary symbols (PM dimensions), as compared to one M-ary symbol (M dimensions), must be decoded jointly. In this case, the nonlinear PPM-specific sphere decoders proposed in [13] must be applied resulting in more complex receivers. Finally, for $M \geq P$, the choice of applying scheme 1 or scheme 2 depends on the complexity constraints on the receiver and on wether $\mathcal{R}_1$ is smaller or greater than $\mathcal{R}_2$. Note that the decoding complexity of scheme 2 is the same as that of [7], [8].

IV. Coverage Extension Offered by the MIMO techniques

The low transmission levels imposed on UWB communications have direct implications on the achieved communication ranges and data rates. In this section, we discuss the coverage extension and the data rate enhancement offered by the diversity schemes that we proposed in the previous section.

Designate by E_b and N_0 the average energy per information bit and the noise spectral density respectively. The ratio E_b/N_0 can be related to the communication distance (d) by [14]:

$$\frac{E_b}{N_0} = EIRP + 10\log_{10}(B) + G_t + G_r - 10\alpha \log_{10}\left(\frac{4\pi f_c d}{c}\right) - 10\log_{10}(R_b) - (-173.83 + F) - I \quad (44)$$

where $EIRP$ is the effective isotropic radiated power, B is the -10 dB bandwidth of the transmitted pulses. G_t and G_r are the gains of the transmit and receive antennas respectively. α is the path loss exponent. If f_{min} and f_{max} stand for the -10 dB edges of the spectrum occupied by the waveforms, then $f_c = \sqrt{f_{min} f_{max}}$. F is the noise figure of the receiver and I is the implementation loss. $R_b = \frac{\mathcal{R}}{N_f T_f}$ is the transmission rate where $\mathcal{R}$ is the number of bits transmitted PCU: $\mathcal{R} = \log_2(M)$ (resp. $\mathcal{R} = M\log_2(P)/P$) for scheme 1 (resp. scheme 2).

V. Simulations and results

We consider FCC-compliant Gaussian pulses occupying the $[3.1\ 5.1]$ GHz bandwidth. In this case, $EIRP = -41.25$ dBm/MHz [1]. In eq. (44), we fix $G_t = G_r = 0$ dB, $F = 6$ dB, $I = 5$ dB and $\alpha = 2$ which corresponds to free-space propagation. The transmit and the receive arrays are supposed to be sufficiently spaced so that each one of the PQ sub-channels is generated independently from the other sub-channels using the standard IEEE 802.15.3a channel model recommendations CM1 and CM2 that correspond to line-of-sight (LOS) and non-line-of-sight (NLOS) conditions [14]. The modulation delay of the PPM constellation is fixed to: $\delta = 0.5$ ns. Since δ is small compared to the channel delay spread (that is in the order of $\Gamma = 100$ ns), all of the presented simulations take IPI into consideration. At the receiver side, perfect channel state information is assumed. A modified version of the sphere decoder is applied [13]. This assures that the output of the decoder corresponds to the closest point of the multi-dimensional PPM constellation (and not simply to the closest lattice point).

In the first simulation setup, we fix $T_f = 100$ ns which is larger than the channel delay spread. Consequently, this setup highlights the diversity and multiplexing advantages of the proposed schemes independently from IFI and ISI. N_f has no effect on the performance in the absence of IFI and ISI and it is fixed to 1.

Fig. 3 compares the performance of single-antenna IR-UWB systems with that of $P \times 1$ MISO-UWB systems using scheme 1 with 5-PPM for $P = 2, 3, 5$. The receiver is equipped with a 4-finger Rake. Results show the enhanced diversity order and the high performance levels achieved by the proposed scheme. In Fig. 4, we compare the performance of scheme 1 with that of the rate-1 shape-preserving code proposed in [8] with 8-PPM. This simulation shows that the diversity order of both codes is the same and that [8] slightly outperforms scheme 1 (by about 0.5 dB at 10^{-3}). However, this enhanced performance is realized at the expense of an increased decoding complexity since [8] necessitates the joint ML detection of P PPM symbols while scheme 1 is symbol-by-symbol decodable. Note that [8] is the best known rate-1 PPM code and that, with respect to this code, scheme 1 compromises a small performance loss with an important reduction in the receiver complexity especially for large numbers of transmit antennas.

In Fig. 5, we compare the two diversity schemes with 16-PPM. The enhanced multiplexing gain of scheme 2 (that reaches 8 bits PCU with 4 transmit antennas compared to 4 bits PCU for scheme 1) manifests itself in high performance

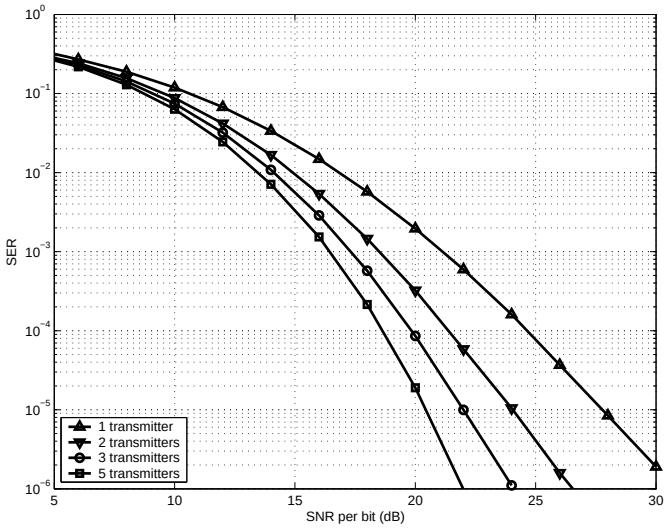

Fig. 3. Performance of scheme 1 on CM2 with 5-PPM. One receive antenna and a 4-finger Rake are used.

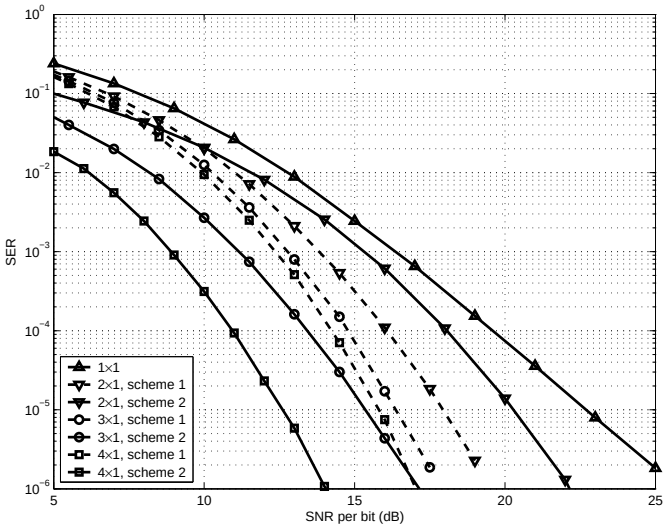

Fig. 5. Scheme 1 versus scheme 2 with 16-PPM. Simulations are performed over CM2 and the receiver is equipped with a 5-finger Rake.

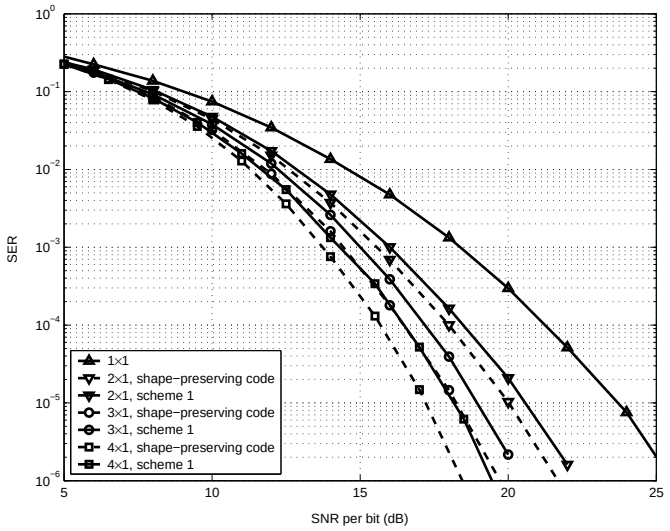

Fig. 4. Scheme 1 versus the rate-1 code in [8] with 8-PPM. Simulations are performed over CM2 and the receiver is equipped with a 4-finger Rake.

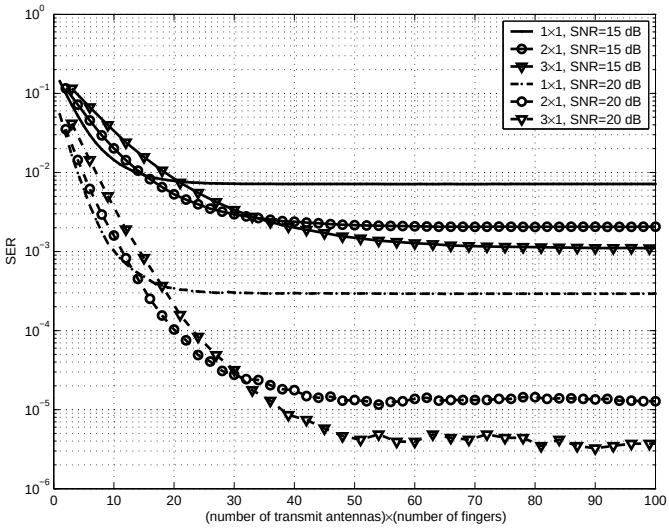

Fig. 6. Transmit diversity versus multi-path diversity with 3-PPM. Scheme 1 is applied in the MIMO case. Simulations are performed over CM2.

levels especially at low SNRs. This figure shows the very high performance levels achieved by scheme 2. The performance enhancements are associated with a higher decoding complexity (which is the same as that of [8]).

To highlight the advantages of ST coding with UWB systems, Fig. 6 compares systems having the same overall diversity order that is equal to the product PQL (with $Q = 1$ in this case). 3-PPM is used and for a fair comparison, we plot the symbol error rates (SER) as a function of PL for SNRs of 15 dB and 20 dB (note that the gap between the 1×1 and $P \times 1$ systems will increase if the SER was plotted as a function of L alone). For example, a 1×1 system equipped with 60 fingers achieves a SER of 3×10^{-4} at a SNR of 20 dB. In this case, the 2×1 system with only 30 fingers achieves a better SER in the order of 10^{-5} while the 3×1 system with 20 fingers achieves a SER of 4×10^{-6}. Fig. 6 shows that exploiting the transmit diversity by increasing the number of transmit antennas can be more beneficial than enhancing the multi-path diversity by increasing the number of Rake fingers even though there is no increase in the energy capture. This follows from the fact that consecutive multi-path components of the same sub-channel can be simultaneously faded because of cluster and channel shadowing [14]. For SNR=20 dB, Fig. 6 shows that it is possible to achieve error rates smaller than 10^{-5} by increasing the number of transmit antennas while it was impossible to reach such error rates with single-antenna systems with any number of Rake fingers.

In Fig. 7, we consider the impact of IFI and ISI. We fix $N_f = 1$ and the frame duration can take the values of $T_f = 8$, 15 or 100 ns. In particular, we compare 2×2 systems employing either scheme 2 or Spatial-Multiplexing (SM) with 16-PPM. The superiority of scheme 2 is evident for all levels of interference. In this scenario, both scheme 2 and SM transmit 8 bits PCU. However, scheme 2 presents

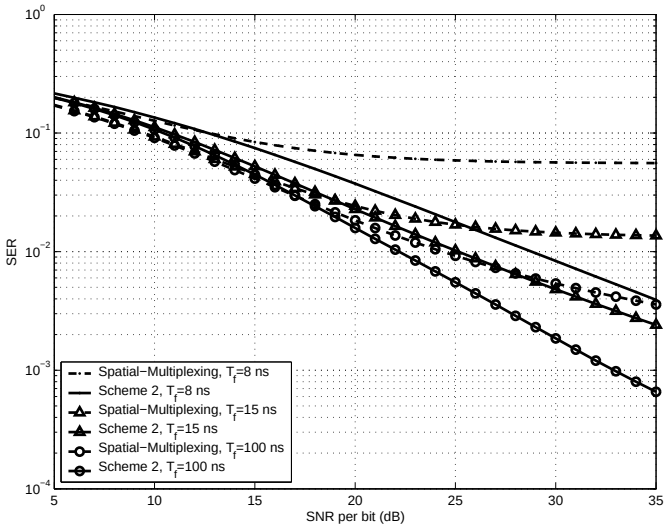

Fig. 7. Scheme 2 versus spatial-multiplexing in the presence of inter-symbol-interference. 2×2 MIMO systems are considered with 16-PPM. The receiver is equipped with a 1-finger Rake.

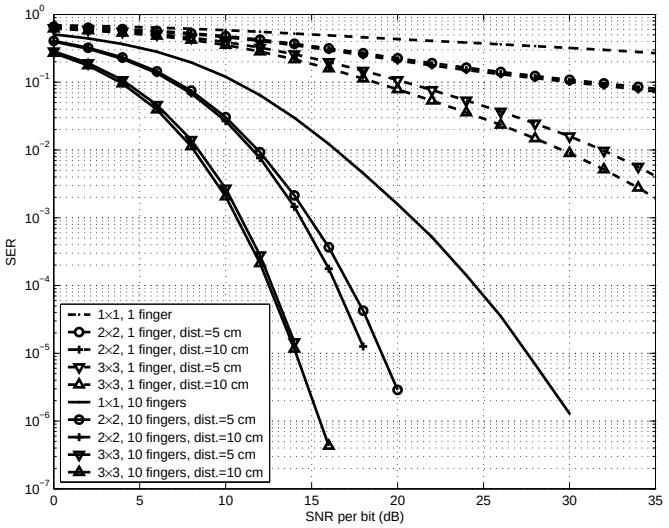

Fig. 9. Performance over the Kunisch-Pamp profile-2 model [15]. Scheme 1 is used with 4-PPM.

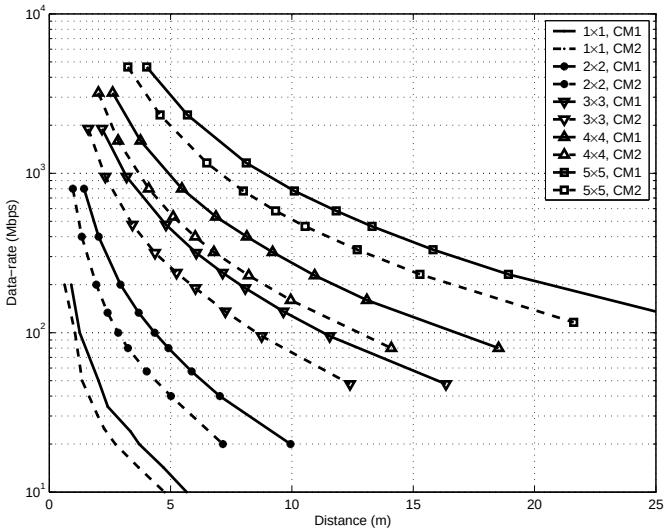

Fig. 8. The achievable data rate as a function of the communication distance at a SER of 10^{-3} with 4-PPM. Results are shown for CM1 and CM2 using a 3-finger Rake.

the additional advantage of being fully diverse. This enhanced diversity results in decreasing the error floors that result from interference. For example, SM has an error floor of 6×10^{-2} for $T_f = 8$ ns while scheme 2 can achieve error rates that are smaller than 10^{-2} while transmitting at the same data-rate of 1 Gbps.

By applying eq. (44), we plot the binary rate R_b as a function of the communication distance d in Fig. 8 for a target SER of 10^{-3}. Scheme 2 is applied with 4-PPM and a 3-finger Rake. We fix $N_f = 4$ while T_f is varied from 2.5 ns to 100 ns. At a first time, the SER is averaged over 10^4 channel realizations by Monte Carlo simulations. At a second time, the value of E_b/N_0 corresponding to a target SER of 10^{-3} is determined and d is calculated from eq. (44). Results show the suitability of the proposed MIMO-UWB solutions for high data-rate WPANs since they can boost the data-rate and (or) the coverage of such networks. For example, while a single-antenna system can not deliver more than 14 Mbps at a distance of 5 m on CM1, the 6×6 system achieves the data rate of about 3 Gbps (without any channel coding).

While all of the previous simulations were performed assuming that the MIMO channels are independent, Fig. 9 shows the performance over the space-variant UWB channel model proposed in [15]. Simulations are performed over profile 2 that corresponds to an office NLOS scenario for antenna array separations of 5 cm and 10 cm. Scheme 1 is applied with 4-PPM. Results show the high performance levels over this realistic MIMO model that takes spatial correlation into consideration. It can be observed that the diversity orders for both array separations are the same with the larger separation resulting only in a slightly better performance.

VI. Conclusion

We presented two novel diversity techniques for IR-MIMO-UWB systems using unipolar PPM constellations. The proposed constructions solve the problem of the non-existence of unipolar codes for any number of transmit antennas and signal-set dimensionality. With respect to single-antenna systems, the proposed schemes add no additional constraints on the RF circuitry to control the amplitude and the phase of the UWB pulses. Results show that data rates in the order of 1 Gbps can be achieved by the proposed schemes for communication distances that do not exceed 5 m thus making the proposed schemes strong candidates for high data-rate WPANs.

Appendix

To simplify the analysis, in the construction of the $(PM \times J)$-dimensional codeword A, instead of stacking $a_{p,j,1}, \ldots, a_{p,j,M}$ vertically for a given value of (p, j), we chose to stack $a_{1,j,m}, \ldots, a_{P,j,m}$ vertically one after the other for a given value of (m, j). In other words, the $((m-1)P+$

$p,j)$-th element of A will be equal to $a_{p,j,m}$. Based on this new formulation, eq. (16) will be written as:

$$\mathcal{Y} = [I_P \otimes (I_M \otimes H)]\,\mathcal{A} + \mathcal{N} \triangleq \mathcal{H}\mathcal{A} + \mathcal{N} \qquad (45)$$

where the constituent elements of the $QL \times P$ matrix H are given in eq. (19).

Based on the encoding scheme described in eq. (41), the P^2M-dimensional vector $\mathcal{A}$ can be written as:

$$\mathcal{A} \triangleq \text{vec}(A) = \Phi S \qquad (46)$$

$$= \left[\begin{array}{cccc} (I_M \otimes I_P)^T & (I_M \otimes \Omega)^T & \cdots & \left(I_M \otimes \Omega^{P-1}\right)^T \end{array}\right]^T \cdot \left[\begin{array}{cccc} e_{s_1}^T & \cdots & e_{s_M}^T \end{array}\right]^T \qquad (47)$$

where $s_1, \ldots, s_M \in \{1, \ldots, P\}$ correspond to the information symbols and Ω is the $P \times P$ matrix given by:

$$\Omega = \left[\begin{array}{cc} \mathbf{0}_{1\times(P-1)} & 1 \\ I_{P-1} & \mathbf{0}_{(P-1)\times 1} \end{array}\right] \qquad (48)$$

The ML criterion is the same as eq. (24) where $\mathcal{H}^T\mathcal{H} = [I_P \otimes (I_M \otimes H)]^T [I_P \otimes (I_M \otimes H)] = I_P \otimes (I_M \otimes G)$ following from the properties of the Kronecker product where $G = H^T H$ is the $P \times P$ matrix whose constituent elements are given in eq. (25).

Following from the structure of matrix Φ given in eq. (47) and from the fact that $\left(\Omega^i\right)^T = \Omega^{-i}$, it can be directly proven that:

$$\Phi^T\mathcal{H}^T\mathcal{H}\Phi = I_M \otimes \left[\sum_{i=1}^{P} \Omega^{-i} G \Omega^i\right] \triangleq I_M \otimes \mathcal{G} \qquad (49)$$

Inspecting the structure of $\mathcal{G}$, it can be proven that its (i,j)-th element can be written as:

$$\mathcal{G}_{i,j} = \sum_{k=0}^{P-1} g_{\sigma^k(i),\sigma^k(j)} \quad ; \quad i,j = 1, \ldots, P \qquad (50)$$

Since the P permutations $\sigma^0(p), \ldots, \sigma^{P-1}(p)$ span the entire set $\{1, \ldots, P\}$ for all values of $p = 1, \ldots, P$, then the diagonal elements of $\mathcal{G}$ are given by ($i = 1, \ldots, P$):

$$\mathcal{G}_{i,i} \triangleq \alpha = \sum_{k=0}^{P-1} g_{\sigma^k(i),\sigma^k(i)} = \sum_{p=1}^{P} g_{p,p} = \sum_{p=1}^{P}\sum_{q=1}^{Q}\sum_{l=1}^{L} h_{q,l,p}^2 \qquad (51)$$

Consequently, for any PM-dimensional information vector S whose structure is described in eq. (47), the scalar $S^T\Phi^T\mathcal{H}^T\mathcal{H}\Phi S$ is always equal to $M\mathcal{G}_{i,i}$ which is a constant implying that this term can be removed from the ML metric given in eq. (24).

Therefore, the decision can be based on the metric $\mathcal{Y}^T\mathcal{H}\Phi S$. Assuming that the vector $S' = [e_{s'_1}^T \ \cdots \ e_{s'_M}^T]^T$ was transmitted, then at high SNR: $\mathcal{Y} = \mathcal{H}\Phi S'$ implying that:

$$\mathcal{Y}^T\mathcal{H}\Phi S = S'^T\Phi^T\mathcal{H}^T\mathcal{H}\Phi S = \sum_{m=1}^{M} \mathcal{G}_{s_m,s'_m} \triangleq \beta_{S,S'} \qquad (52)$$

From eq. (51) and eq. (52), it follows that for a correct decision by the ML decoder, $\beta_{S',S'} = M\alpha = M\sum_{p,q,l} h_{q,l,p}^2$ implying that the L fingers of all of the PQ MIMO sub-channels add up coherently and that the system profits from full transmit, receiver and multi-path diversity orders.

For $S \neq S'$, combining equations (50) and (52) results in:

$$\beta_{S,S'} = \sum_{m=1}^{M}\sum_{k=0}^{P-1} g_{\sigma^k(s_m),\sigma^k(s'_m)} = \sum_{m=1}^{M}\sum_{k=0}^{P-1}\sum_{q=1}^{Q}\sum_{l=1}^{L} h_{q,l,\sigma^k(s_m)} h_{q,l,\sigma^k(s'_m)} \qquad (53)$$

Note that for $s_m \neq s'_m$, $\sigma^k(s_m) \neq \sigma^k(s'_m)$ implying that $\sum_{k=0}^{P-1} g_{\sigma^k(s_m),\sigma^k(s'_m)} \leq \sum_{k=0}^{P-1} g_{\sigma^k(s_m),\sigma^k(s_m)} = \alpha$ following from the properties of the autocorrelation function. Consequently, an erroneous estimated position s_m will result in cross terms that do not add up coherently in $\beta_{S,S'}$ and that are smaller than α. Consequently, the imposed diversity order enhances the useful information-bearing part of the received signal without increasing the probability of confusing it with other signals corresponding to different information symbols.

Note that in the absence of IPI, the block-diagonal structure of the matrix $\Phi^T\mathcal{H}^T\mathcal{H}\Phi$ in eq. (49) insures that the symbols $s_1, \ldots, s_M$ can be decoded separately. This is not the case in the presence of IPI where these symbols must be decoded jointly. Once again, IPI results in cross-product terms that do not add up coherently and, consequently, do not affect the overall diversity order of the system. These interference terms become more and more negligible compared to $\beta_{S',S'} = M\sum_{p,q,l} h_{q,l,p}^2$ (corresponding to a correct decision) as M, P, Q or L increase.

REFERENCES

[1] F. C. Commission, "First report and order, technical report FCC 02-48," www.fcc.gov., April 2002.

[2] L. Yang and G. B. Giannakis, "Analog space-time coding for multi-antenna ultra-wideband transmissions," *IEEE Trans. Commun.*, vol. 52, pp. 507–517, March 2004.

[3] E. Baccarelli, M. Biagi, C. Pelizzoni, and P. Bellotti, "A novel multi-antenna impulse radio UWB transceiver for broadband high-throughput 4G WLANs," *IEEE Commun. Lett.*, vol. 8, pp. 419 – 421, July 2004.

[4] L. Huaping, R. C. Qiu, and T. Zhi, "Error performance of pulse-based ultra-wideband MIMO systems over indoor wireless channels," *IEEE Trans. Wireless Commun.*, vol. 4, pp. 2939–2944, November 2005.

[5] L. C. Wang, W. C. Liu, and K. J. Shieh, "On the performance of using multiple transmit and receive antennas in pulse-based ultrawideband systems," *IEEE Trans. Wireless Commun.*, vol. 4, pp. 2738–2750, November 2005.

[6] C. Abou-Rjeily and J.-C. Belfiore, "On space-time coding with pulse position and amplitude modulations for time-hopping ultra-wideband systems," *IEEE Trans. Inform. Theory*, vol. 53, no. 7, pp. 2490–2509, July 2007.

[7] ——, "A space-time coded MIMO TH-UWB transceiver with binary pulse position modulation," *IEEE Commun. Lett.*, vol. 11, no. 6, pp. 522–524, June 2007.

[8] C. Abou-Rjeily and W. Fawaz, "Space-time codes for MIMO ultra-wideband communications and MIMO free-space optical communications with PPM," *IEEE J. Select. Areas Commun.*, vol. 26, no. 6, pp. 938–947, August 2008.

[9] S. M. Alamouti, "A simple transmit diversity technique for wireless communications," *IEEE J. Select. Areas Commun.*, vol. 16, pp. 1451–1458, October 1998.

[10] B. A. Sethuraman, B. S. Rajan, and V. Shashidhar, "Full-diversity, high rate space-time block codes from division algebras," *IEEE Trans. Inform. Theory*, vol. 49, pp. 2596–2616, October 2003.

[11] F. Oggier, G. Rekaya, J.-C. Belfiore, and E. Viterbo, "Perfect space time block codes," *IEEE Trans. Inform. Theory*, vol. 52, no. 9, pp. 3885 – 3902, September 2006.

[12] M. K. Simon and V. A. Vilnrotter, "Alamouti-type space-time coding for free-space optical communication with direct detection," *IEEE Trans. Wireless Commun.*, vol. 4, pp. 35–39, January 2005.
[13] C. Abou-Rjeily, "A maximum-likelihood decoder for joint pulse position and amplitude modulations," in *Proceedings IEEE Int. Conf. on Personal, Indoor and Mobile Radio Commun.*, September 2007, pp. 1–5.
[14] J. Foerster, "Channel modeling sub-committee Report Final," Technical report IEEE 802.15-02/490, IEEE 802.15.3a WPANs, 2002.
[15] J. Kunisch and J. Pamp, "An ultra-wideband space-variant multipath indoor radio channel model," in *Proceedings IEEE Conf. on UWB Systems and Technologies*, November 2003, pp. 290 – 294.